The recurrent *SET-NUP214* fusion as a new *HOXA* activation mechanism in pediatric T-cell acute lymphoblastic leukemia

Pieter Van Vlierberghe,[1] Martine van Grotel,[1] Joëlle Tchinda,[2] Charles Lee,[2] H. Berna Beverloo,[3] Peter J. van der Spek,[4] Andrew Stubbs,[4] Jan Cools,[5] Kyosuke Nagata,[6] Maarten Fornerod,[7] Jessica Buijs-Gladdines,[1] Martin Horstmann,[8] Elisabeth R. van Wering,[9] Jean Soulier,[10] Rob Pieters,[1] and Jules P. P. Meijerink[1]

[1]Department of Pediatric Oncology/Hematology, Erasmus Medical Center (MC) Sophia Children's Hospital, Rotterdam, The Netherlands; [2]Department of Pathology, Brigham and Women's Hospital, Harvard Medical School, Boston, MA; [3]Department of Clinical Genetics, Erasmus MC, Rotterdam, The Netherlands; [4]Department of Bioinformatics, Erasmus MC, Rotterdam, The Netherlands; [5]Department of Molecular and Developmental Genetics, Flanders Interuniversity Institute for Biotechnology (VIB), University of Leuven, Leuven, Belgium; [6]Department of Infection Biology, Graduate School of Comprehensive Human Sciences and Institute of Basic Medical Sciences, University of Tsukuba, Tsukuba, Japan; [7]Department of Tumor Biology, The Netherlands Cancer Institute, Amsterdam, The Netherlands; [8]German Co-operative Study Group for Childhood Acute Lymphoblastic Leukemia (COALL), Hamburg, Germany; and [9]Dutch Childhood Oncology Group (DCOG), The Hague, The Netherlands; and [10]Hematology Laboratory, Hôpital Saint-Louis, Paris, France

T-cell acute lymphoblastic leukemia (T-ALL) is mostly characterized by specific chromosomal abnormalities, some occurring in a mutually exclusive manner that possibly delineate specific T-ALL subgroups. One subgroup, including *MLL*-rearranged, *CALM-AF10* or inv (7)(p15q34) patients, is characterized by elevated expression of *HOXA* genes. Using a gene expression–based clustering analysis of 67 T-ALL cases with recurrent molecular genetic abnormalities and 25 samples lacking apparent aberrations, we identified 5 new patients with elevated *HOXA* levels. Using microarray-based comparative genomic hybridization (array-CGH), a cryptic and recurrent deletion, del (9)(q34.11q34.13), was exclusively identified in 3 of these 5 patients. This deletion results in a conserved SET-NUP214 fusion product, which was also identified in the T-ALL cell line LOUCY. SET-NUP214 binds in the promoter regions of specific *HOXA* genes, where it interacts with CRM1 and DOT1L, which may transcriptionally activate specific members of the *HOXA* cluster. Targeted inhibition of SET-NUP214 by siRNA abolished expression of *HOXA* genes, inhibited proliferation, and induced differentiation in LOUCY but not in other T-ALL lines. We conclude that SET-NUP214 may contribute to the pathogenesis of T-ALL by enforcing T-cell differentiation arrest. (Blood. 2008;111:4668-4680)

Introduction

T-cell acute lymphoblastic leukemia (T-ALL) is a thymocyte malignancy, and represents about 15% of pediatric patients with ALL. T-ALL often presents with a high tumor mass, accompanied by a rapid progression of disease. Still, about 30% of patients with T-ALL relapse during therapy or within the first 2 years following treatment and eventually die.[1]

Over the last few years, great progress has been made in unravelling the genetics of T-ALL, including recurrent chromosomal translocations (*TAL1*, *LYL1*, *LMO1*, *LMO2*, *HOX11*/*TLX1*, *HOX11L2*/*TLX3*, *MYB*, and *Cyclin D2*), deletions (*SIL-TAL1*, del(6q), del(9)(p21), and del(11)(p12p13)), amplifications (*NUP214-ABL1*), duplications (*MYB*), and mutations (*RAS* and *NOTCH1*).[2-13] Some of these abnormalities are mutually exclusive and may delineate distinct T-ALL subgroups (ie, *TAL1*, *LMO1*, *LMO2*, *HOX11*, *HOX11L2*, *CALM-AF10*, *MLL*, and Inv(7)). Others are shared by some of these subgroups and may lead to the deregulation of cell cycle (ie, del(9)(p21) that includes the *CDKN2A/p15* and *CDKN2B/p16* loci).[3,4] Some may be acquired during leukemic growth, like the episomal *NUP214-ABL1* amplification.[6] *NOTCH1* activation mutations are present in more than half of all patients with T-ALL regardless of the presence of other rearrangements.[7] It has been hypothesized that activation of *NOTCH1* represents one of the most advanced abnormalities in T-ALL that may enable for uncontrolled proliferation and/or inhibition of apoptosis, possibly through up-regulation of the target genes *cMYC* and *DELTEX1*.[14-16]

In contrast to the wide variety of genetic abnormalities in T-ALL, initial microarray studies have revealed only 5 different expression clusters: immature/*LYL1*, *TAL1*, *HOX11*, *HOX11L2*, and *HOXA* clusters.[8,17] One of the explanations for this phenomenon is that patients with different molecular cytogenetic defects may share a highly similar expression profile and are being recognized as one single expression cluster.[8,17] For example, patients with different abnormalities demonstrate high expression of genes of the *HOXA* cluster (*HOXA5*, *-A9*, *-A10*, and *-A11*). This cluster includes patients with *CALM-AF10*[8,18] or *MLL* rearrangements,[8,19] or patients with an inversion on chromosome 7 due to the rearrangement of the T-cell receptor-beta (*TCRβ*) locus into the *HOXA* cluster.[8,10] Elevated *HOXA* gene expression levels have also been reported in the absence of these genetic aberrations,[8,20] suggesting that alternative mechanisms of *HOXA* activation may exist in T-ALL.

Previously, we have studied the incidence and prognostic relevance of recurrent molecular cytogenetic abnormalities for pediatric T-ALL.[21] Within our cohort, about half of the patients

Submitted September 10, 2007; accepted February 12, 2008. Prepublished online as *Blood* First Edition paper, February 25, 2008; DOI 10.1182/blood-2007-09-111872.

The online version of this article contains a data supplement.

The publication costs of this article were defrayed in part by page charge payment. Therefore, and solely to indicate this fact, this article is hereby marked "advertisement" in accordance with 18 USC section 1734.

with T-ALL lack currently known molecular cytogenetic abnormalities. To identify the underlying genetic defects in these patients, we used various high-resolution genomic screening strategies, including microarray-based comparative genomic hybridization (array-CGH). We recently described a new and recurrent deletion (ie, the del(11)(p12p13)), in about 4% of patients with T-ALL.[12] This interstitial deletion leads to the loss of a negative regulatory domain upstream of *LMO2*, resulting in ectopic expression of this oncogene. Array-CGH also led to the identification of a recurrent duplication of *MYB* in about 10% of patients with T-ALL.[2,9]

In this study, we combined gene expression profiling and array-CGH analysis to detect a new and recurrent molecular cytogenetic abnormality in patients with T-ALL that coclustered with 5 well-defined *HOXA*-activated T-ALL samples. We describe the cloning of a recurrent *SET-NUP214* fusion product in these samples, and identified a potential mechanism by which *SET-NUP214* may activate the *HOXA* gene cluster as potential leukemogenic event in T-ALL.

Methods

Patient samples

Viably frozen diagnostic bone marrow or peripheral blood samples from 92 pediatric patients with T-ALL and clinical and immunophenotypic data were provided by the German Cooperative Study Group for Childhood Acute Lymphoblastic Leukemia (COALL) and the Dutch Childhood Oncology Group (DCOG). The patients' parents or their legal guardians provided informed consent to use leftover material for research purposes in accordance with the Declaration of Helsinki. The Review Board of the Erasmus Medical Center approved the use of human participants in this study. Leukemic cells were isolated and enriched from these samples as previously described.[12] All resulting samples contained 90% or more leukemic cells, as determined morphologically by May-Grünwald-Giemsa–stained cytospins (Merck, Darmstadt, Germany). Viably frozen T-ALL cells were used for DNA and RNA extraction, and a minimum of 5×10^6 leukemic cells were lysed in Trizol reagent (Invitrogen, Life Technologies, Breda, The Netherlands) and stored at −80°C. A total of 25×10^3 leukemic cells was used to prepare cytospin slides for fluorescence in situ hybridization (FISH) and stored at −20°C.

Genomic DNA isolation, RNA extraction, and cDNA synthesis

Genomic DNA and total cellular RNA were isolated using Trizol (Invitrogen) according to the manufacturer's protocol, with minor modifications. An additional phenol-chloroform extraction was performed, and the RNA was precipitated with isopropanol along with 1 μL (20 μg/mL) glycogen (Roche, Almere, The Netherlands). After precipitation, RNA pellets were dissolved in 20 μL RNAse-free TE buffer (10 mM Tris-HCl, 1 mM EDTA [pH 8.0]). The RNA concentration was quantified spectrophotometrically. Following a denaturation step of 5 minutes at 70°C, 1 μg RNA was reverse transcribed to single-stranded cDNA using a mix of random hexamers (2.5 μM) and oligodT primers (20 nM). The reverse transcriptase (RT) reaction was performed in a total volume of 25 μL containing 0.2 mM of each dNTP (Amersham Pharmacia Biotech, Piscataway, NJ), 200 U Moloney murine leukemia virus (M-MLV) RT (Promega, Madison, WI), and 25 U RNAsin (Promega). Conditions for the RT reaction were 37°C for 30 minutes, 42°C for 15 minutes, and 94°C for 5 minutes. The cDNA was diluted to a final concentration of 8 ng/μL and stored at −80°C.

Gene expression array analysis

Integrity of total RNA was checked using the Agilent 2100 Bio-analyzer (Agilent, Santa Clara, CA). Copy DNA and ccRNA syntheses from total RNA, hybridization of Humane Genome U133 plus 2.0 oligonucleotide microarrays (Affymetrix, Santa Clara, CA), and washing steps were performed according to the manufacturers' protocols. Probeset intensities were extracted from CEL files using GeneChip Operating Software (GCOS) version 1.4.0.036 (Affymetrix), and all arrays had a 3′ end to 5′ end GAPDH ratio lower than 3-fold. Probe intensities were normalized using the variance stabilization procedure (Bioconductor package VSN[22]; http://www.bioconductor.org/) in the statistical data analysis environment *R*, version 2.2.0 (http://www.r-project.org/). Differentially expressed genes between T-ALL subgroups were calculated using a Wilcoxon statistical test, and corrected for multiple testing error according to the false discovery rate procedure as developed by Hochberg and Benjaminin[23] using the Bioconductor package Multtest. The fold change was calculated using the formula: $e^{(\text{median value group A} - \text{median value group B})}$. Supervised clustering and principal component analyses were performed using GeneMath XT 1.6.1 software (Applied Maths, Austin, TX).

Array-CGH

Array-CGH analysis was performed, as previously described,[12,24] on the human genome CGH Microarray 44A (Agilent), which consists of approximately 40 000 60-mer oligonucleotide probes that span both coding and noncoding sequences with an average spatial resolution of approximately 35 kb. Briefly, 10 μg genomic reference or patient DNA was digested overnight at 37°C with *Alu*I (20 U) and *Rsa*I (20 U; Invitrogen). Reference and patient DNA were purified and labeled with Cy5-dUTP and Cy3-dUTP (PerkinElmer, Wellesley, MA). Reference and patient DNA for each hybridization were pooled and mixed with 50 μg human Cot-1 DNA (Invitrogen), 100 μg yeast tRNA (Invitrogen), and 1 × hybridization control targets (SP310; Operon Technologies, Alameda, CA) in a final volume of 500 μL in situ hybridization buffer (Agilent). The hybridization mixtures was denatured at 95°C for 3 minutes, preincubated at 37°C for 30 minutes, and hybridized to the array in a microarray hybridization chamber (Agilent) for 14 to 18 hours at 65°C in a rotating oven (Robbins Scientific, Mountain View, CA) at 20 rpm. The array slides were washed in 0.5 × SSC/0.005% Triton X-102 at room temperature for 5 minutes, followed by 5 minutes at 37°C in 0.1 × SSC/0.005% Triton X-102. Slides were dried and scanned using a 2565AA DNA microarray scanner (Agilent). Microarray images were analyzed using feature extraction software (version 8.1; Agilent), and the data were subsequently imported into array-CGH analytics software v3.1.28 (Agilent). Microarray data are available at http://www.ncbi.nlm.nih.gov/geo/ (accession no. GSE10609).

FISH

FISH analysis was performed on thawed cytospin slides using the LSI BCR-ABL ES translocation probe, according to the manufacturer's protocol (Vysis, Downers Grove, IL). Cells were counterstained with DAPI/Vectashield mounting medium (Vysis). Fluorescence signals were visualized with a Zeiss Axioplan II fluorescence microscope (Zeiss, Sliedrecht, The Netherlands) using Mac Probe Software (version 4.3, Applied Imaging, Newcastle upon tyne, United Kingdom). The combined presence of a clonal del(9)(q34.11q34.13) and an episomal *NUP214-ABL1* amplification in patient no. 120 was determined by FISH analysis as previously described[12] using bacterial artificial chromosomes (BACs) clones RP11-83J21 (covering *ABL1*) and RP11-618A20 (covering *ASS1*, located in the deleted area between *SET* and *ABL1*). BACs were obtained from BAC/PAC Resource Center (Children's Hospital, Oakland, CA).

RT-PCR and RQ-PCR

The *SET-NUP214* fusions were determined by RT–polymerase chain reaction (PCR) using forward primer 5′-TTCCCGATATGGATGATG-3′ (exon 7 *SET*) and reverse primer 5′-CTTTGGGCAAGGATTTG-3′ (exon 20 *NUP214*). PCR reactions were performed using 40 ng cDNA (8 ng/μL), 10 pmol primers, 10 nmol dNTPs, 4 mM $MgCl_2$, 1.25 U ampli*Taq* gold (Applied Biosystems, Foster City, CA) in 10 × PCR buffer II (Applied Biosystems) in a total volume of 50 μL. After the initial denaturation at 94°C for 10 minutes, PCR was performed for 39 cycles of 95°C for 15 seconds, 60°C for 1 minute, and 68°C for 3 minutes. *NUP214-ABL1* fusions were determined as previously described.[6]

Expression levels of *HOXA, SET*, and *SET-NUP214* transcripts were quantified relative to the expression level of the endogenous housekeeping gene glyceraldehyde-3-phosphate dehydrogenase (*GAPDH*) using quantitative RT-PCR (RQ-PCR) in an ABI 7700 sequence detection system (Applied Biosystems). The *HOXA* primers were as described previously.[8] For *SET* expression, the forward primer 5′-TTCCCGATATGGATGATG-3′ (exon 7 *SET*) and the reverse primer 5′-CCCCCCAAATAAATTGAG-3′ (exon 8 *SET*) were used. For *SET-NUP214* expression, the primers used were as described in "RT-PCR and RQ-PCR."

Cell culture

T-ALL cell lines (DSMZ, Braunschweig, Germany) were cultured in RPMI-1640 medium (Invitrogen) supplemented with 10% fetal calf serum (Integro, Zaandam, The Netherlands), 100 IU/mL penicillin, 100 μg/mL streptomycin, and 0.125 μg/mL fungizone (Invitrogen) and grown as suspension cultures at 37°C in humidified air containing 5% CO_2. LOUCY and SKW3 cells (10^7) were transfected with 50 nM *SET* siRNA by electroporation in 400 μL RPMI 1640 with L-alanyl-L-glutamine (Invitrogen) in 4 mm electroporation cuvettes (BioRad, Hercules, CA). The SET siRNAs were located in exon 5 (5′-GAAAUCAAAUGGAAAUCUGGAAA-3′), exon 3 (5′-CGAGUCAAACGCAGAAUAA-3′), and exon 8 (5′-AGGAGAAGAUGACUAAAUA-3′). To compensate for the amount of cell death induced as a consequence of the electroporation procedure, control cells were electroporated without siRNA. Electroporation was performed using an EPI 2500 gene pulser (Fischer, Heidelberg, Germany) applying a rectangle pulse of 350 V for 10 ms. After incubating for 15 minutes at room temperature, the cells were diluted 10-fold with RPMI 1640 medium (Invitrogen) supplemented with 10% FCS (Integro), 100 IU/mL penicillin, 100 μg/mL streptomycin, and 0.125 μg/mL fungizone (Invitrogen) and incubated at 37°C and 5% CO_2. Cell viability was assessed by annexinV/propidium iodide (PI) staining and determined by flow cytometry using a FACSCalibur (Becton Dickinson, San Jose, CA). Electroporation of a fluorescein isothiocyanate (FITC)–labeled siRNA (Eurogentec, Seraing, Belgium) and subsequent fluorescence-activated cell sorter (FACS) analysis indicated that transfection efficiencies were greater than 90%. Electroporation of this FITC-labeled siRNA also served as negative siRNA control.

Immunophenotyping and cell-cycle analysis was performed by multicolor flow cytometry using an LSR II flow cytometer (BD Biosciences, Franklin Lakes, NJ). A total of 2 different 6-color labeling combinations were performed: labeling 1, anti-TCRαβ (FITC), anti-TCRγδ (peridine chlorophyll protein [PE]), CD3 (phycoerythrin [PerCP]), CD4 (PE-Cy7), CD7 (allophycocyanin [APC]), and CD8 (APC-Cy7); labeling 2, CD3 (FITC), CD10 (PE), CD45 (PerCP), CyCD3 (PE-Cy7), CD5 (APC), and CD2 (APC-Cy7). Data analysis was performed using FACSDiva software version 4.1.2 (BD Biosciences).

Protein extraction and Western blot analysis

Cell pellets stored at −80°C were briefly thawed and resuspended in 50 μL lysis buffer composed of 50 mM Tris buffer, 150 mM NaCl, 100 mM EDTA, 1% Triton X-100, 2 mM PMSF, 3% aprotinine (Sigma, Zwijndrecht, The Netherlands), 4 g/mL pepstatin (Sigma), and 4 μg/mL leupeptin (Sigma). Accordingly, cells were lysed for 15 minutes on ice. The supernatant of the lysed cells was cleared by centrifugation for 15 minutes at 13 000*g* and 4°C. The protein content of the cleared lysates was determined using the BCA protein assay (Pierce Biotechnology, Rockford, IL) with different concentrations of bovine serum albumin as standards. Cell lysates containing 25 μg protein were separated on 10% polyacrylamide gels topped with 4% stacking gels, and transferred onto nitrocellulose membranes (Schleichler & Schuell, Dassel, Germany). Western blots were probed with mouse anti-SET (provided by K.N.) or with mouse antiactin (Sigma) antiserum. Anti-SET was used in different concentrations for proper detection of both SET (1:1000) and SET-NUP214 (1:250). Accordingly, the blots were labeled with peroxidase-conjugated anti-mouse IgG antibodies (DAKO, Glostrup, Denmark) and visualized using SuperSignal West Femto chemiluminescent substrate (Pierce Biotechnology).

IP and ChIP

For chromatin immunoprecipitation (ChIP) analysis, 20×10^6 cells were crosslinked using formaldehyde to a final concentration of 1% for 15 minutes at room temperature. Cross-linking was stopped by adding glycine to a final concentration of 0.125 M followed by 5 minutes of incubation at room temperature. Fixed cells were washed twice using ice-cold 1 × PBS and harvested in SDS buffer (100 mM NaCl, 50 mM Tris-HCl [pH 8.1], 5 mM EDTA [pH 8.0], 0.2% NaN_3, and protease inhibitors). After centrifugation, the pellet was resuspended in immunoprecipitation (IP) buffer (100 mM Tris [pH 8.6], 0.3% SDS, 1.7% Triton X-100, and 5 mM EDTA), and the cells were sonicated yielding genomic DNA fragments with a size of 500 to 1000 bp. After preclearing the lysates with protein A beads (50% slurry protein A–Sepharose; Upstate, Charlottesville, VA), the samples were immunoprecipitated overnight at 4°C with affinity-purified anti-NUP214 antibodies (provided by M.F.[25]), antidimethyl H3K79 (Upstate), antiacetylated H3 (Upstate) or anti-FLAG (Sigma). The immune complexes were recovered by adding 50 μL protein A beads and were incubated for 2 hours at 4°C. Subsequently, beads were washed with low-salt buffer (0.1% SDS, 1% Triton X-100, 2 mM EDTA, 20 mM Tris-HCl [pH 8.1], and 150 mM NaCl), high-salt buffer (0.1% SDS, 1% Triton X-100, 2 mM EDTA, 20 mM Tris-HCl [pH 8.1], and 500 mM NaCL), LiCl buffer (250 mM LiCl, 1 mM EDTA, 0.5% NP-40, 10 mM Tris-HCL [pH 8.0], and 0.2% NaN_3), and 1 × TE buffer (10 mM Tris-HCL [pH 8.0], and 1 mM EDTA). The immune complexes were eluted from the beads by adding elution buffer (1% SDS and 0.1M $NaHCO_3$) for 15 minutes at room temperature. Cross-links were reversed by overnight incubation at 65°C. The eluted material was phenol/chloroform-extracted and ethanol-precipitated. The immunoprecipitated DNA was quantified by RQ-PCR using *HOXA*-specific promoter primers as previously described.[26]

For IP analysis, cells were washed twice using ice-cold 1 × PBS and lysed in a single-detergent lysis buffer (142.5 mM KCl, 5 mM $MgCl_2$, 10 mM HEPES [pH 7.0], 1 mM EDTA, 1% NP-40, and protease inhibitors). After preclearing the lysates with protein A beads (Upstate), samples were immunoprecipitated overnight at 4°C with rabbit anti-NUP214, rabbit anti-PP32 (gift from Dr J. Brody, Johns Hopkins University, Baltimore, MD), mouse anti-SET, rabbit anti-CRM1 (gift from Dr M. Yoshida, University of Tokyo, Japan), and rabbit anti-hDOT1L (gift from Dr Yi Zhang, Lineberger Cancer Center, Chapel Hill, NC). The immune complexes were recovered by adding 50 μL protein A beads and were incubated for 2 hours at 4°C. Subsequently, beads were washed twice by single-detergent lysis buffer and twice by single-detergent lysis buffer without NP-40. The pellets were resuspended in loading buffer and boiled for 5 minutes, and Western blot analysis was performed as described in "Protein extraction and Western blot analysis."

Results

Gene expression profiling of pediatric T-ALL subgroups

We have used gene expression profiling data to cluster 92 patients with T-ALL: 67 patients with known cytogenetic abnormalities and 25 patients without recurrent aberrations (from this point denoted as unknown patients). For the 67 patients with T-ALL who have one of the major molecular cytogenetic abnormalities (ie, *TAL1* [n = 24], *LMO2* [n = 9], *HOXA* [n = 5], *HOX11/TLX1* [n = 7], and *HOX11L2/TLX3* [n = 22]), differentially expressed probesets were calculated from Affymetrix U133 plus 2.0 data based upon a Wilcoxon analysis and corrected for multiple testing for each probeset. Significant and differentially expressed probesets were obtained for the *TAL1*, *HOX11*, and *HOX11L2* subgroups (Figure 1A). No significant probesets were obtained for the *HOXA* subgroup or the *LMO2* subgroup (Figure 1A). As *TAL1* and *LMO2* both participate in the same transcriptional complex,[27] activation of these genes may both lead to a highly similar expression profile.

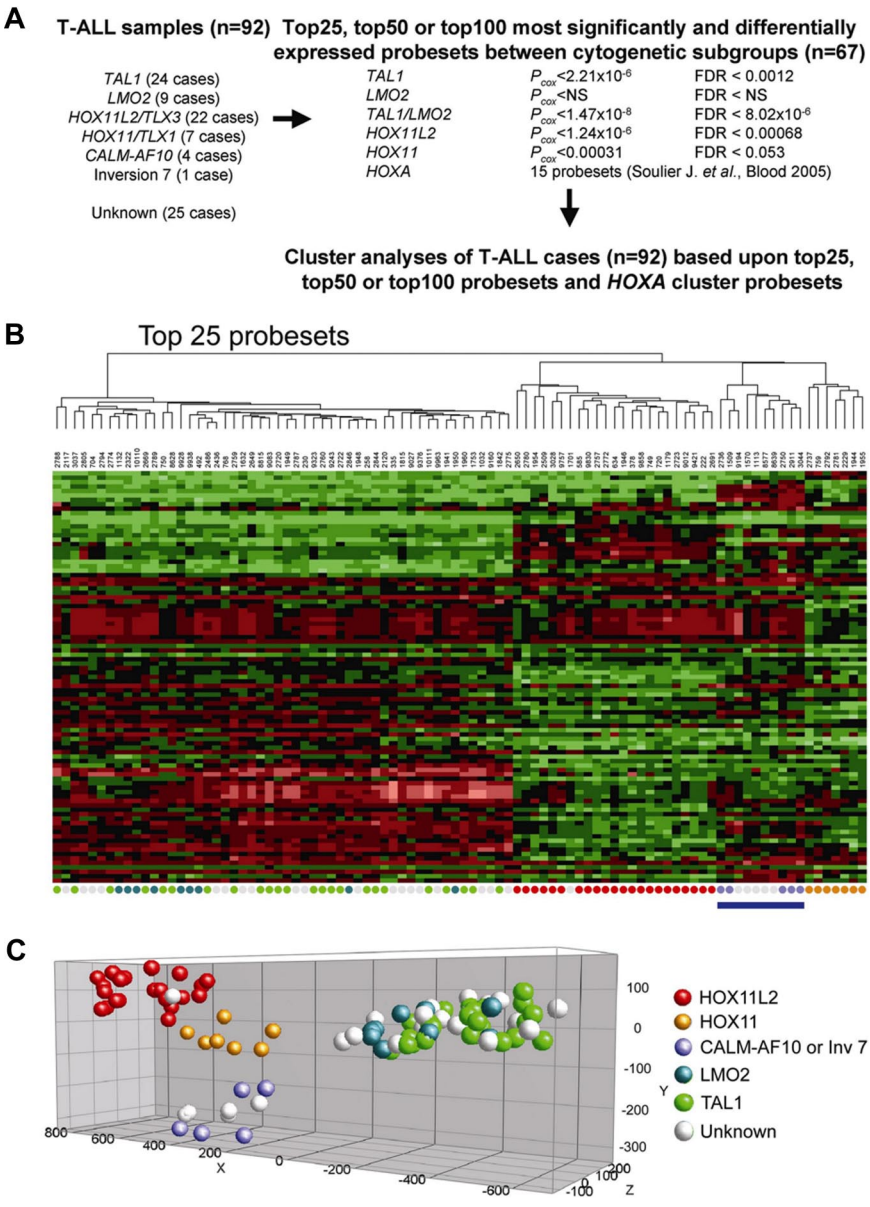

Figure 1. Gene expression profiles of 92 T-ALL patients. (A) Differentially expressed genes among the major molecular cytogenetic T-ALL subgroups (*TAL1*, *LMO2*, *HOXA*, *HOX11/TLX1*, and *HOX11L2/TLX3*; n = 67). The significance level (Wilcoxon *P* value) and FDR corrected *P* value for the top 100 genes in each T-ALL subgroup is indicated. *TAL1*, *HOX11*, and *HOX11L2* subgroups show significant differentially expressed probesets. (B) Cluster analysis of 92 patients with T-ALL (67 with known, 25 with unknown) based upon the top 25 most significant probesets for the *TAL1*, *TAL1/LMO2*, *HOX11*, and *HOX11L2* subgroups combined with 15 *HOXA* probesets as previously described.[8] (C) Principal component analyses shows clustering of the patients with unknown T-ALL along the molecular cytogenetic known patients: 1 *HOX11L2*-like, 19 *TAL1/LMO2*-like, and 5 *HOXA*-like patients.

Combined analysis of *TAL1*- and *LMO2*-rearranged patients revealed significant and differentially expressed probesets that, as expected, almost entirely overlapped with the gene signature obtained for the *TAL1* subgroup only.

Next, we tried to cluster all 92 patients with T-ALL. Cluster analysis was performed based upon the top 25, 50, or 100 most significant probesets for the *TAL1*, *TAL1/LMO2*, *HOX11*, and *HOX11L2* subgroups combined with 15 *HOXA* probesets identified by Soulier et al[8] (Table S1, available on the *Blood* website; see the Supplemental Materials link at the top of the online article; Figure 1A,B). Cluster and principal component analyses (PCAs) led to a stable clustering of patients with unknown T-ALL with specific molecular cytogenetic subgroups (Figure 1B,C; Figure S1; Table S2): one patient clustered with *HOX11L2*-rearranged patients, and this patient uniquely highly expressed the *HOX11L2* homologous gene *HOX11L1* (data not shown). A total of 19 unknown patients tightly clustered with *TAL1*- or *LMO2*-rearranged patients. FISH analysis (not shown) revealed *TAL1* and/or *LMO2* homologous rearrangements to the *TCRβ* or *TCRαδ* loci in 5 of these 19 patients (ie, *TAL2* [1 patient]; *LMO1* [1 patient]; *TAL2/LMO1* [1 patient]; and *cMYC* [2 patients] in line with karyotypic data. Another 5 unknown T-ALL samples formed a separate cluster with the 5 patients with *HOXA*-type T-ALL (Figure 1B,C; Table S2), and will be denoted as *HOXA*-like samples.

New recurrent deletion, del(9)(q34.11q34.13), in *HOXA*-like T-ALL samples

To identify new chromosomal abnormalities in the 5 *HOXA*-like patients, we screened these patients using oligonucleotide array-CGH. A one-copy loss of an approximately 3-Mb region involving chromosomal band 9q34.11 to 9q34.13 was identified in 3 of 5 *HOXA*-like patients (patient nos. 126, 125, and 120; Figure 2A-C). Detailed analysis of the centromeric breakpoints in these 3 patients revealed a breakpoint within or in the vicinity of the *SET* gene. The *PKN3* gene just telomeric to *SET* was consistently lost in all 3 patients (Figure 2A-C). The telomeric breakpoint was located in the *NUP214/CAN* gene in 2 patients (nos. 125 and 126; Figure 2A-C), whereas the telomeric

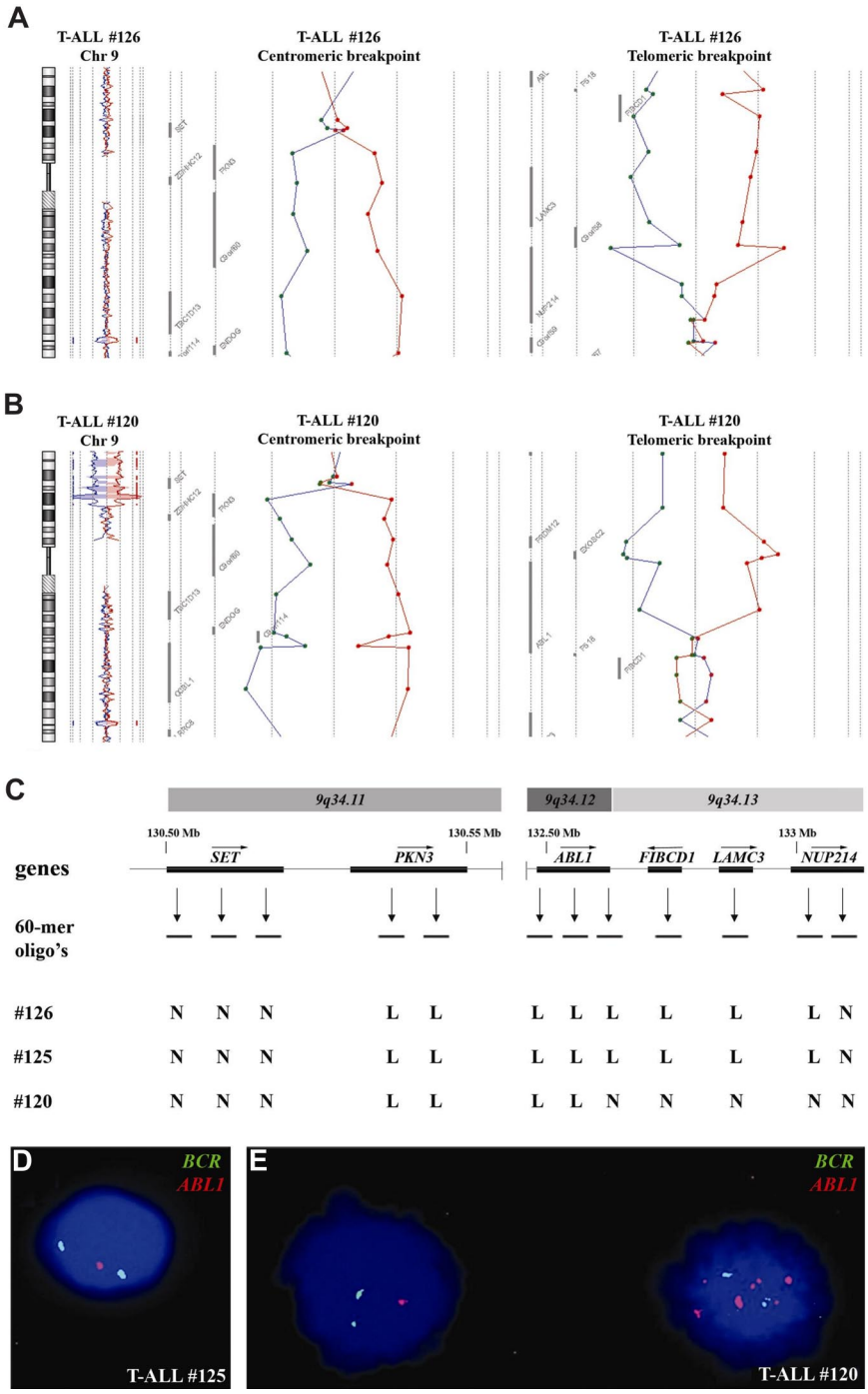

Figure 2. Submicroscopic del(9)(q34.11q34.13) in T-ALL. (A) Chromosome 9 ideogram and corresponding oligo array-CGH plots of test DNA–control DNA ratios (blue tracing) versus the dye-swap experiment (red tracing) for patient no. 126. Detailed analyses of the centromeric and telomeric breakpoints show involvement of *SET* and *NUP214*. (B) Similar array-CGH plot for patient no. 120. Centromeric and telomeric breakpoints show involvement of *SET* and *ABL1*. (C) Overview of oligoarray-CGH results in the potential breakpoint regions for 3 patients with T-ALL with del(9)(q34.11q34.13). The 60-mer oligonucleotide probes present on the array-CGH slide and located in the telomeric and centromeric breakpoint regions, as well as the specific genes located in this region with their transcription direction, are shown. Abbreviations: N; normal, L; loss. Dual-color FISH analysis of patient no. 125 (D) and no. 120 (E) using the LSI *BCR-ABL* ES translocation probe.

breakpoint of patient no. 120 seemed situated in the *ABL1* oncogene (Figure 2B,C).

The presence of the del(9)(q34.11q34.13) in patient nos. 125 and 126 was confirmed by FISH using the LSI *BCR-ABL* ES translocation probe, resulting in a single-copy loss of the *ABL1* gene (Figure 2D). Strikingly, FISH analysis on patient no. 120 also revealed an identical monoallelic loss of *ABL1* in all leukemic cells. However, an episomal *NUP214-ABL1* amplification[6] was detected in a leukemic subclone comprising approximately 5% of the total leukemic cell population (Figure 2E). Subsequent FISH analysis confirmed that the episomal *NUP214-ABL1* amplification as well as the del(9)(q34.11q34.13) were both present in this subclone (data not shown). The combined presence of a clonal del(9)(q34.11q34.13) in combination with an episomal *NUP214-ABL1* amplification in a leukemic subclone in this patient explains why the telomeric breakpoint of the del(9)(q34.11q34.13) seemed situated in the *ABL1* gene according to the array-CGH data. Additional FISH screening of the remaining 87 patients with T-ALL did not reveal other patients with this same deletion.

SET-NUP214 fusion in del(9)(q34.11q34.13)$^+$ patients

Subsequent RT-PCR analysis to amplify a potential *SET-NUP214* fusion product using a *SET* forward primer (exon 7) in combination with a *NUP214* reverse primer (exon 20) revealed an *SET-NUP214* fusion product in all 3 del(9)(q34.11q34.13)$^+$ patients with T-ALL that we also identified in the T-ALL cell

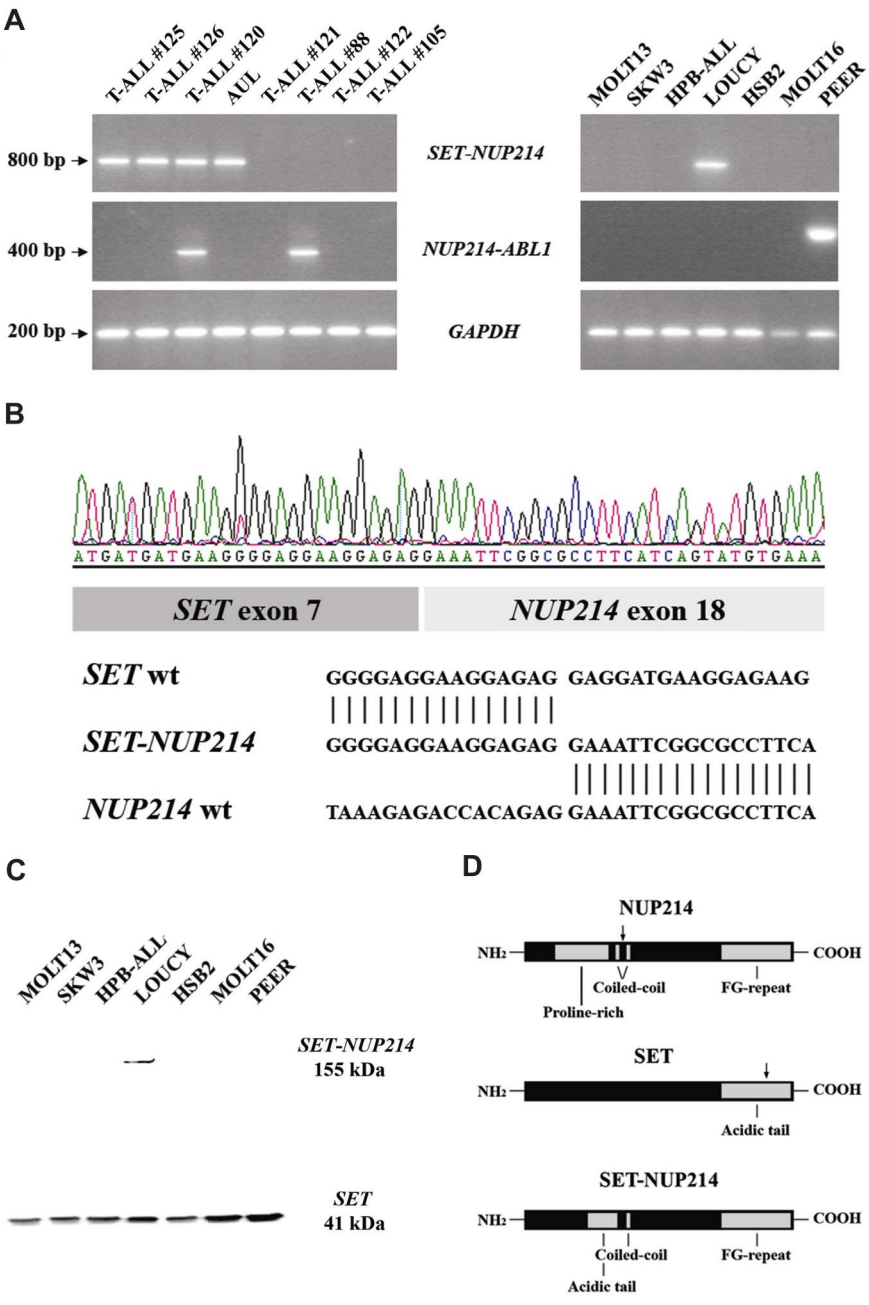

Figure 3. SET-*NUP214* fusion transcript in T-ALL. (A) RT-PCR analysis using *SET*- and *NUP214*-specific primers and *GAPDH* primers as internal control, reveals a specific *SET-NUP214* fusion gene in T-ALL patient nos. 125, 126, and 120; the patient with AUL; and the T-ALL cell line LOUCY. *NUP214-ABL1* fusion was detected in patient nos. 120 and no.88 and in the T-ALL cell line PEER (B) Sequence analysis confirmed an identical fusion between exon 7 of *SET* and exon 18 of *NUP214* in all *SET-NUP214*$^+$ patients with T-ALL, the patient with AUL, and the LOUCY cell line. (C) Western blot analysis of T-ALL cell lines revealed a SET-NUP214 fusion in the cell line LOUCY. (D) At the protein level, the breakpoints are situated in the acidic tail of SET and the coiled-coil domain of NUP214.

line LOUCY[28] (Figure 3A). A similar *SET-NUP214* fusion product due to the reciprocal chromosomal translocation t(9;9)(q34;q34) has been described previously for a patient with an acute undifferentiated leukemia (AUL) by Von Lindern et al.[29] Material from this patient with AUL was still available, and RT-PCR analysis revealed a *SET-NUP214* fusion product in this patient (Figure 3A). Sequence analyses of the *SET-NUP214* PCR products confirmed that these 3 patients with T-ALL and the patient with AUL,[29] as well as the cell line LOUCY, all had an identical fusion product fusing *SET* at exon 7 with the *NUP214* gene at exon 18 (Figure 3B). Additional oligonucleotide array-CGH analysis further confirmed that the *SET-NUP214* fusion in the LOUCY cell line was indeed due to the presence of a del(9)(q34.11q34.13). This deletion was not present in the patient with AUL, confirming that the *SET-NUP214* fusion was the result of a balanced t(9;9)(q34;q34) in this patient.[29]

RT-PCR analysis also confirmed an episomal *NUP214-ABL1* fusion product present in patient no. 120, as well as in control patient material with an episomal *NUP214-ABL1* amplification (Figure 3A; patient no. 88). Sequence analysis confirmed an in-frame fusion of *NUP214* exon 31 to exon 2 of *ABL1* for patient no. 120.

As expected, the presence of a SET-NUP214 fusion protein was detected by Western blotting in LOUCY (Figures 3C), but was absent in other T-ALL cell lines lacking the del(9)(q34.11q34.13). For all patients described, the breakpoints are situated in the acidic tail of SET and the coiled-coil domain of NUP214, generating an in-frame fusion protein with a molecular weight of approximately 155 kDa (Figure 3D).

Clinical and genetic patient characteristics (ie, *NOTCH1* mutation status and additional aberrations detected by array-CGH) of the *SET-NUP214*$^+$ patients with T-ALL and the LOUCY cell line are summarized in Table 1.

Table 1. Characteristics of 3 patients with T-ALL and the T-ALL cell line LOUCY with the *SET-NUP214* fusion transcript

Patient no.	Sex	Age, y	WBC, $\times 10^9$/L	Blasts, %	Immune phenotype*	CDKN2A†	NOTCH1 mutation	NUP214-ABL1	Other chromosomal abnormalities by array-CGH	Relapse CCR, mo
126	F	15.3	213	98	Mature	+/+	L1601Q	−	None	CCR,83+
125	F	10.6	142	94	Mature	+/+	L1601P	−	del(16)(p13.13)	CCR,83+
120	F	17.1	15	93	Cortical	−/−	N1683D, Q2460*(stop)	+	del(9)(p21.2), monosomy 21	CCR,37+
LOUCY	F	38	NA	NA	Mature	+/−	ND	−	del(5)(q14.3q31.1), del(5)(q33.1), del(6)(q16.4), del(9)(p21.2p21.3), del(12)(p13.1p13.3), dup(13)(q31.3), del(16)(p12.3)	NA

WBC indicates white blood cells; CCR, continued complete remission; ND, none detected; and NA, not available.
*According to the European Group of Immunological Characterisation of Leukemia (EGIL) classification.
†Status of the CDKN2A locus: +/+, no deletion; +/−, hemizygous deletion; −/−, homozygous deletion.

Elevated HOXA levels in SET-NUP214$^+$ patients

To confirm the clustering of these 3 del(9)(q34.11;q34.13)$^+$ patients within the *HOXA* cluster based upon the most significant and differentially expressed probesets between the major T-ALL subgroups, we analyzed the expression of the *HOXA* gene cluster using RQ-PCR. As a control, we also determined the expression levels for these genes in various other patient samples representing other T-ALL subgroups. As described previously,[8,10,18,19] *MLL*-rearranged cases (n = 2), *CALM-AF10*$^+$ cases (n = 4), and a patient with an inv(7)(p15q34) mutation all highly expressed most genes from the *HOXA* cluster in contrast to *TAL1*-, *LMO2*-, *HOX11L2*-, or *HOX11*-rearranged patients ($P < .01$; Figure 4A,B; only results for *HOXA9* are shown). All 3 *SET-NUP214*$^+$ patients with T-ALL as well as the LOUCY cell line also highly expressed the *HOXA* cluster of genes. Other T-ALL cell lines, including MOLT13, SKW3, HPB-ALL, HSB2, and PEER, did not express the *HOXA* gene cluster. Although most *HOXA* genes were highly expressed in LOUCY, in the patient with AUL and in the *SET-NUP214*$^+$ patients with T-ALL, expression of *HOXA11* and *HOXA13* was virtually absent. In addition, the expression of the short *HOXA10* isoform, *HOXA10B*, which previously has been exclusively associated with patients with inv(7)(p15q34) T-ALL,[8,20] was also highly expressed in the *SET-NUP214*$^+$ patients (Figure 4C).

From the expression microarray data, the most significant and differentially expressed probesets were calculated for the entire *HOXA* cluster. A total of 20 significant and differentially expressed probesets with a FDR rate lower than 5% were obtained for this cluster (Figure 4D). Various of these probesets encoding for *QKI*, *HOXA5*, *HOXA9* (2 probesets), *HOXA10* (2 probesets), and *HOXA11* were also previously found to be differentially expressed within *MLL*-rearranged[19] or *CALM-AF10*–rearranged[18] patients with T-ALL or in patients with T-ALL belonging to the *HOXA* subgroup.[8]

SET-NUP214 activates *HOXA* expression, increases cellular proliferation, and inhibits cellular differentiation

To study the role of the *SET-NUP214* fusion transcript in the pathogenesis of T-cell leukemia and its contribution to the activation of the *HOXA* gene cluster, *SET* and *SET-NUP214* expression were specifically down-regulated in the LOUCY cell line by electroporation of *SET*-specific siRNAs (Figure 5). Protein expression of SET and SET-NUP214 was specifically reduced using a *SET* siRNA directed against exon 5, whereas only SET but not SET-NUP214 was down-regulated using a *SET* siRNA directed against exon 8 (Figure 5A). *SET* and/or *SET-NUP214* mRNA expression levels were specifically targeted, and this effect was sustained for more than 7 days following transfection of *SET* siRNAs (Figure 5B). Specific down-regulation of both SET and SET-NUP214 resulted in significant reduction in the expression levels of the *HOXA* gene cluster, while knockdown of SET but not SET-NUP214 had no effect (Figure 5C). This confirms that SET-NUP214, or the combination of SET and SET-NUP214, specifically up-regulates the expression of *HOXA* genes. Knockdown of SET-NUP214 also reduced cellular proliferation (Figure 5D,E), but the percentage of apoptotic cells did not change over time following inhibition of SET-NUP214 (Figure 5F). In addition, SET-NUP214 down-regulation resulted in the up-regulation of both TCRγδ and membrane CD3 expression in LOUCY (Figure 5G), indicating that repression of SET-NUP214 enforces differentiation. Down-regulation of SET by anti-SET siRNA exon 8 had no effect (Figure 5G). The effects of *SET-NUP214* knockdown (*HOXA* inhibition, mild reduced cell proliferation, and induction of differentiation) were confirmed using a second *SET* siRNA directed against exon 3 (Figure S3).

SET-NUP214 directly activated *HOXA* expression, possibly by recruitment of DOT1L

Our siRNA-mediated knockdown experiments indicated that SET-NUP214 regulates the transcription of the *HOXA* gene cluster. To investigate whether this activation was caused by direct interaction of SET-NUP214 with *HOXA* promoter sequences, ChIP analyses with the LOUCY cell line and the negative control cell line SKW3 were performed. No enrichment of *HOXA* (*HOXA1*, *HOXA3*, *HOXA9*, *HOXA10*, and *HOXA11*) promoter sequences was detected in NUP214 immunoprecipitates obtained for SKW3 control cells (Figure 6A). For LOUCY cells, *HOXA9* and *HOXA10* promoter sequences were enriched in NUP214 immunoprecipitates, but not *HOXA1*, *HOXA3*, and *HOXA11* promoter sequences, indicating that SET-NUP214 may only bind to specific members of the *HOXA* cluster (Figure 6A). Enrichment of *HOXA9* and *HOXA10* promoter sequences in the ChIP analysis could be completely reversed using *SET* siRNA molecules directed against exon 5.

Additional ChIP analysis using antiacetyl histone H3 (Figure S2)– and antidimethyl histone H3K79 (Figure 6A)–specific antibodies revealed histone H3 acetylation and histone H3K79 methylation of *HOXA1*, *HOXA3*, *HOXA9*, *HOXA10* and *HOXA11* promoters in

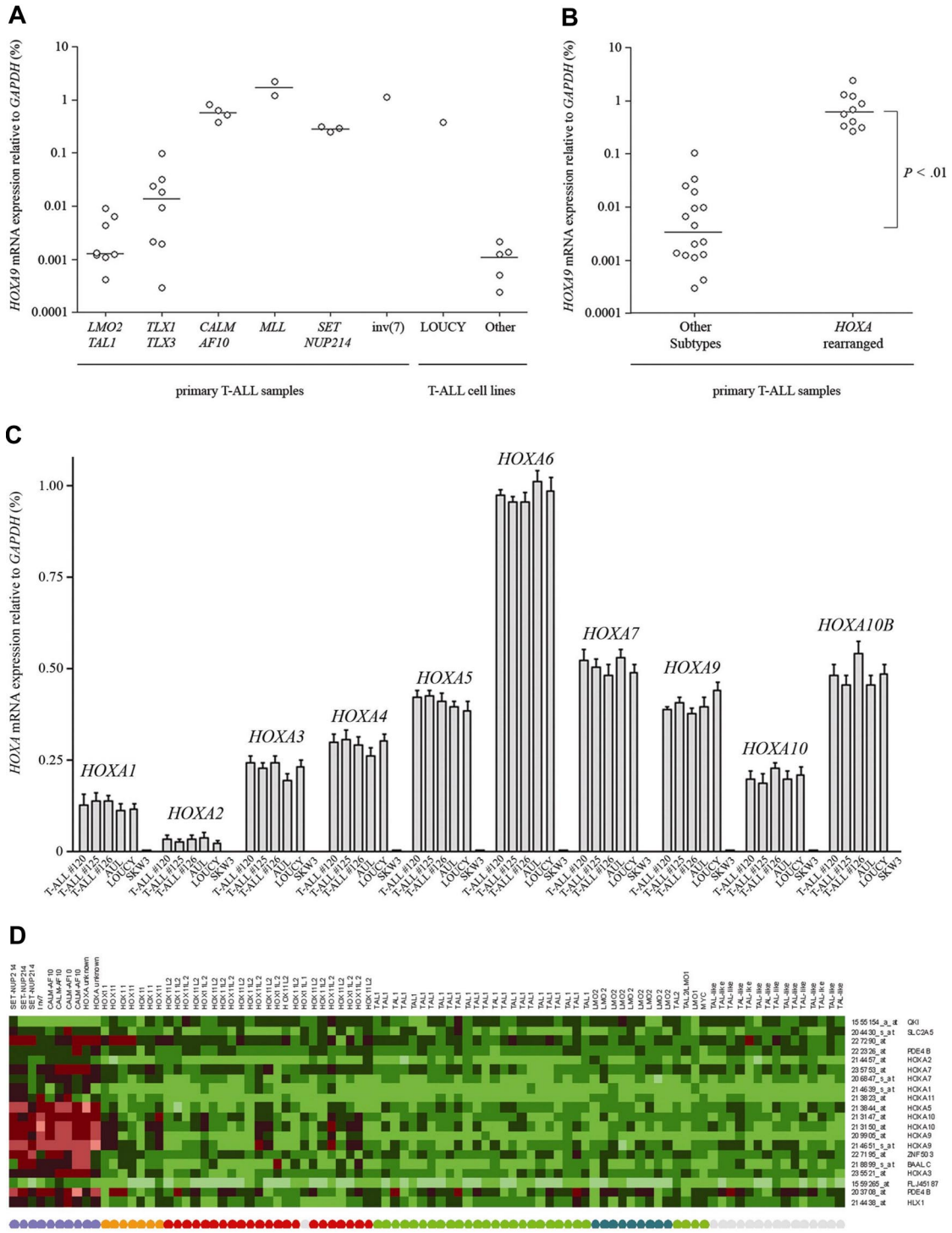

Figure 4. HOXA activation in *SET-NUP214*$^+$ T-ALL. (A) Relative *HOXA9* expression levels by RQ-PCR for *MLL*-rearranged, *CALM-AF1*0^+, inv(7)(p15q34), *TAL1*-, *LMO2*-, *HOX11L2*-, or *HOX11*-rearranged patients and T-ALL cell lines including LOUCY, MOLT13, SKW3, HPB-ALL, HSB2, and PEER. (B) Comparison of *HOXA9* expression levels between the *HOXA* T-ALL subgroup (*MLL*, *CALM-AF10*, inv(7)(p15q34), and SET-NUP214; n = 10) and other T-ALL subgroups (*TAL1*, *LMO2*, *HOX11L2*, or *HOX11*). The horizontal lines represent the medians. (C) Relative expression levels of *HOXA* genes by RQ-PCR for the 3 *SET-NUP214*$^+$ patients with T-ALL, the LOUCY cell line, the patient with AUL, and SKW3. (D) Heatmap of the 20 significant and differentially expressed probesets with a false discovery rate (FDR) lower than 5% for the *HOXA* cluster compared with the other patients with T-ALL.

the LOUCY cell line, which was absent in SKW3. This further strengthens the idea that binding of SET-NUP214 as a specific transcriptional cofactor for some *HOXA* gene members may result in an open chromatine structure of the entire *HOXA* cluster. Upon *SET-NUP214* inactivation, the histone H3K79 methylation was partially lost (Figure 6A), indicating that sustained histone H3K79 methylation of the HOXA locus depended on the presence of SET-NUP214. The level off histone H3 acetylation of the *HOXA* locus remained unaltered within the time frame of the experiment (Figure S2). As SET normally associates with the *HOXA* gene cluster[30] and has an inhibitory role on gene transcription as part of the INHAT complex,[31] we investigated whether SET-NUP214 may

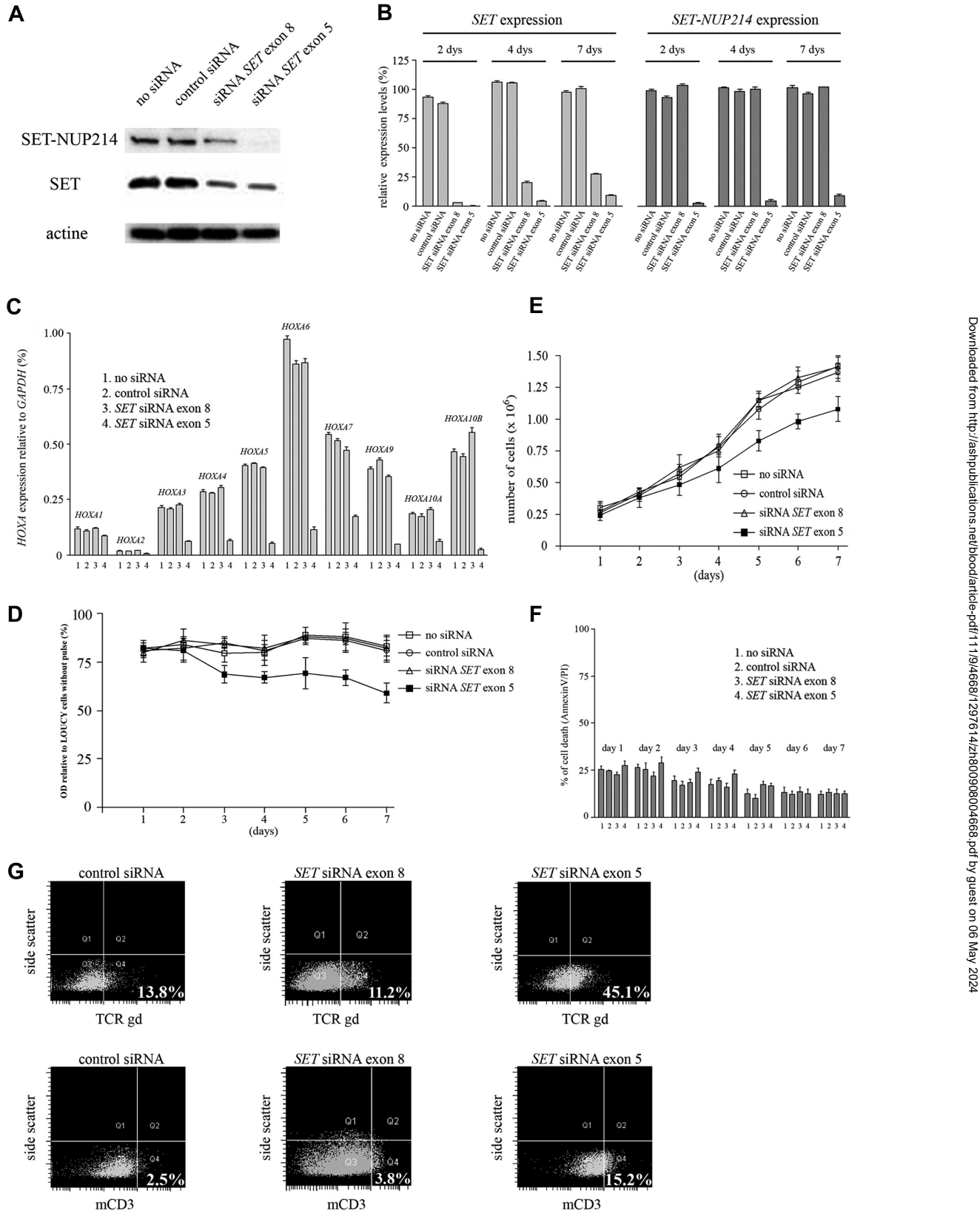

Figure 5. siRNA knockdown of SET and SET-NUP214 in the LOUCY T-ALL cell line. (A) SET expression using Western blot analysis 4 days after electroporation with the following conditions: no siRNA, control siRNA, siRNA *SET* exon 8, or siRNA *SET* exon 5. (B) Relative *SET* and *SET-NUP214* expression by RQ-PCR after 2, 4, and 7 days for conditions as mentioned in panel A. (C) Relative expression of all members of the *HOXA* clusters by RQ-PCR (except for *HOXA11* and *HOXA13*) after 4 days for conditions as mentioned in panel A. (D) Optical density (OD) values relative to control cells without pulse after 7 days for conditions as mentioned in panel A. (E) Total cell numbers after 7 days for conditions as mentioned in panel A. (F) Percentage of cell death relative to control cells without pulse after 7 days for conditions as mentioned in panel A. Error bars visualize the standard error of the mean (SEM). (G) FACS analysis 6 days after electroporation with either no siRNA, siRNA *SET* exon 8, or siRNA *SET* exon 5 for TCRγδ and membrane CD3. The percentage of cells positive for TCRγδ or mCD3 expression are visualized in quadrant 4.

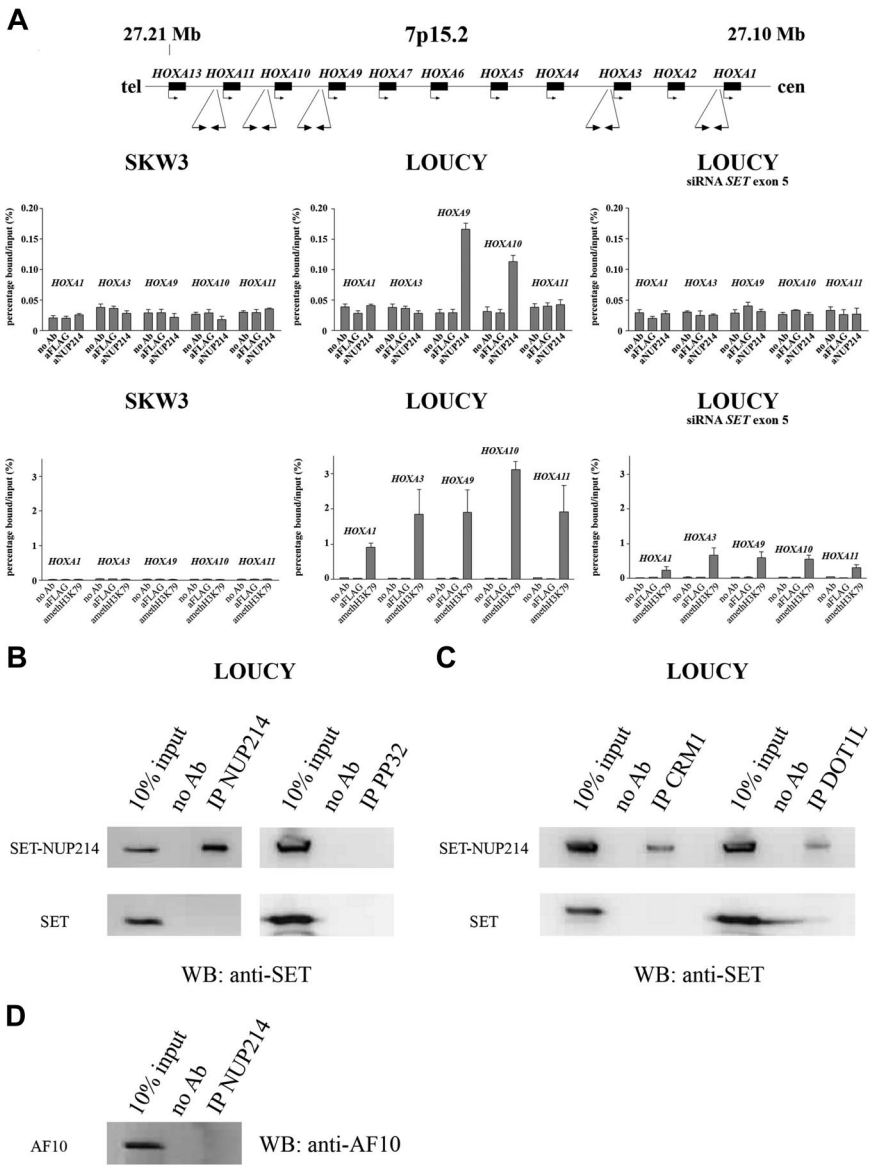

Figure 6. ChIP and coIP analysis of T-ALL cell lines LOUCY and SKW3. (A) ChIP analysis of SKW3, LOUCY, and LOUCY 4 days after electroporation with siRNA *SET* exon 5, for promoter sequences of *HOXA1*, *HOXA3*, *HOXA9*, *HOXA10*, and *HOXA11*. The amount of bound DNA was calculated relative to the 5% input DNA in anti-NUP214 and anti-acetyl histone H3 immunoprecipitates, whereas no antibody and anti-FLAG immunoprecipitates were used as negative control. Error bars represent SEM. (B) Western blot analysis of NUP214 and PP32 immunoprecipitates of the cell line LOUCY using anti-SET. (C) Similar Western blot analysis as in panel B for CRM1 and DOT1L immunoprecipitates in LOUCY. (D) Western blot analysis of NUP214 immunoprecipitates of the cell line LOUCY using anti-AF10.

substitute for SET in this complex, rendering this complex inactive. However, IP experiments failed to demonstrate a direct interaction between SET-NUP214 and components of the INHAT complex (ie, SET and PP32; Figure 6B).

CALM-AF10, *MLL-AF10*, *MLL-ENL*, and *MLL-AF4* fusion proteins have been shown to recruit the methyltransferase DOT1L, leading to aberrant methylation of histone H3 at lysine 79, thereby facilitating transcriptional activation of the *HOXA* gene cluster.[32-35] For CALM-AF10 and MLL-AF10, this interaction with DOT1L depends on the octapeptide and leucine zipper domain (OM-LZ region) in the AF10 part of these fusion proteins.[32,33] With respect to the histone H3–K79 methylation of the *HOXA* locus in our SET-NUP214$^+$ patients, we could demonstrate an interaction between SET-NUP214 and DOT1L in vivo (Figure 6C). However, this interaction seemed independent of the presence of AF10, since an interaction between SET-NUP24 and AF10 could not be demonstrated in LOUCY (Figure 6D). Reciprocal DOT1L IP experiments to study AF10 involvement could not be performed, as suitable DOT1L antibodies for IP experiments are not available. Whether the interaction between DOT1L and SET-NUP214 is a direct interaction or depends on the participation of additional proteins remains to be established. As shown by others,[36,37] we could confirm an in vivo interaction between SET-NUP214 and CRM1 (Figure 6C), which normally binds to the FG-repeat of wild-type NUP214 as part of the nuclear pore complex.[36]

Discussion

Gene expression profiling studies in T-ALL have shown that patients with a *CALM-AF10* translocation, an *MLL* rearrangement, or an inv(7)(p15q34) mutation share a gene expression signature characterized by elevated expression levels of *HOXA* genes. Cluster analysis of 25 patients with T-ALL lacking known cytogenetic abnormalities with 67 cytogenetically well-characterized patients led to the identification of 5 patients with unknown disease that clustered with *HOXA*-activated samples having *CALM-AF10* translocations or an inv(7)(p15q34) mutation.

Subsequent array-CGH analysis revealed an identical interstitial deletion on chromosome 9 [ie, the del(9)(q34.11q34.13)], in

3 of 5 patients as a novel chromosomal aberration in pediatric T-ALL that we also identified in the T-ALL cell line LOUCY. This deletion gives rise to a similar *SET-NUP214* fusion gene in all cases, and was identical to a SET-NUP214 fusion as described 15 years ago for a single acute undifferentiated leukemia patient with a reciprocal translocation t(9;9)(q34;q34),[29,38] and most recently for a single patient with acute myeloid leukemia.[39]

We studied the role of SET-NUP214 in the pathogenesis of T-ALL by siRNA-mediated knockdown of SET-NUP214 in the LOUCY cell line. Down-regulation of SET-NUP214 reduced *HOXA* expression levels, indicating that SET-NUP214 could function as a transcriptional regulator of the *HOXA* gene cluster. Our ChIP data in fact provide evidence that SET-NUP214 directly interacts with the promotor regions of specific *HOXA* members itself, especially with *HOXA9* and *HOXA10,* and therefore may function as a transcriptional coactivator. SET-NUP214 does not bind to promotor sequences of *HOXA1*, *HOXA3*, *HOXA11*, and possibly others despite their SET-NUP214 dependency for transcriptional activation in LOUCY. Binding of SET-NUP214 to *HOXA9* and *HOXA10* promoter regions presumably may lead to an open chromatin structure and transcriptional activation of the entire *HOXA* cluster.

Based upon the ChIP analyses using antiacetylated histone H3 and antidimethyl histone H3–K79 before and after siRNA-mediated SET-NUP214 knockdown, we hypothesize that binding of SET-NUP214 at the *HOXA* promoters may facilitate the recruitment of the H3–K79 methyltransferase DOT1L, resulting in local H3–K79 methylation as a first direct chromatine modification effect. This was supported by our data, in which histone H3–K79 methylation of the *HOXA* locus was partially lost upon inhibition of SET-NUP214 within the (limited) time frame of the experiment. This modification may further trigger the acquisition of other "open state" chromatin modifications, such as H3-acetylation possibly enabling the recruitment of other transcriptional cofactors and transcriptional activation of various *HOXA* gene members.

For MLL-AF10 and CALM-AF10 fusion proteins, it has already been demonstrated that the oncogenicity of these proteins depends on binding of DOT1L to the OM-LZ region of AF10.[32,33] MLL-AF10 and CALM-AF10 both bind to the promoter regions of the *HOXA* gene cluster, and it was shown that recruitment of DOT1L results in aberrant methylation of Lys79 in histone H3 and transcriptional activation of especially *HOXA9* for MLL-AF10[33] and *HOXA5* for CALM-AF10.[32] In addition, recent reports also show interaction of DOT1L with the fusion proteins MLL-ENL and MLL-AF4.[34,35] Our data suggest that *HOXA9* may also represent a bona fide target of the CALM-AF10 fusion protein, as *HOXA9* is highly expressed in CALM-AF10$^+$ T-ALL cells (Dik et al[18] and this study). We propose a similar mechanism for SET-NUP214 in the activation of *HOXA* genes, and *HOXA9*/*HOXA10* in particular, as we could demonstrate binding of DOT1L to the SET-NUP214 fusion protein. An OM-LZ region as present in AF10[33] was not identified in SET-NUP214, and therefore another OM-LZ–like region in SET-NUP214 or an indirect interaction between SET-NUP214 and DOT1L may be facilitated by other SET-NUP214–interacting proteins. In this respect, we confirmed that CRM1 also binds to SET-NUP214,[37] possibly to the FG repeats as retained in this fusion protein.

SET-NUP214 is highly similar to the DEK-NUP214 fusion as previously identified in t(6;9)(p23;q34)$^+$ patients with AML.[40] As DEK-NUP214 AML samples also have an activated *HOXA* gene signature (P. J. Valk, oral communication, January 2008), DEK-NUP214 may function in a similar fashion compared with SET-NUP214 by binding to the promotor regions of specific *HOXA* gene members in t(6;9)(p23;q34)$^+$ patients with AML.

SiRNA knockdown experiments in LOUCY led to complete absence of SET-NUP214 and down-regulation of *HOXA* expression levels that sustained for more than 7 days. Ablation of SET-NUP214 had a mild effect on cellular proliferation without inducing apparent apoptosis in this timeframe. In fact, inhibition of SET-NUP214 may have resulted in cellular differentiation and promoted mCD3 and TCRγδ expression. Our results are in agreement with previous data by others in which overexpression of SET-NUP214 inhibits differentiation in vitro[41] as well as in vivo.[42]

During normal T-cell development, *HOXA* expression (*HOXA7*, *HOXA9*, *HOXA10*) is restricted to the earliest stages of differentiation.[43,44] We therefore propose that SET-NUP214 will sustain *HOXA* gene expression and therefore impair T-cell differentiation. This differentiation arrest may encourage the acquisition of additional genetic hits, eventually leading toward the development of T-cell leukemia. In mouse studies, overexpression of *Hoxa10* inhibits both myeloid and lymphoid cell differentiation,[45] whereas overexpression of *Hoxa9* results in defective T-cell development.[46]

T-cell leukemia depends on multistep pathogenic events.[3-5] Cooperative genetic abnormalities affecting cell cycle and proliferation, differentiation, and survival initiate leukemic transformation of thymocytes. Since *SET-NUP214* fails to cause T-ALL in transgenic mice,[42,47] additional mutations will be required for the induction of T-cell leukemia. We identified a number of cooperative aberrations in the *SET-NUP214*$^+$ T-ALL samples. *NOTCH1* mutations, generally present in about 50% of T-ALL,[7] were found in all 3 *SET-NUP214*$^+$ T-ALL samples. Besides the *SET-NUP214* fusion (differentiation arrest) and *NOTCH1* mutations, patient no. 120 also showed a homozygous *CDKN2A/CDKN2B* deletion (cell-cycle defect) and an episomal *NUP214-ABL1* amplification (proliferation and survival), showing the multiple molecular pathways that are involved in the pathogenesis of T-ALL.[4] It is remarkable that in this patient, 2 different genetic rearrangements (*SET-NUP214* and *NUP214-ABL1*) target the same gene (*NUP214*) in a single leukemic cell. The SET-NUP214 fusion was present as a clonal genetic rearrangement present in all leukemic cells, whereas NUP214-ABL was only present in a leukemic subclone. So SET-NUP214 probably acts as a primary oncogenic event, whereas NUP214-ABL1 rather functions as a further dedifferentiating event in T-ALL. In patient no. 125 and the LOUCY cell line, terminal deletions of chromosome 16 were identified (Table 1). Because these 16p deletions were not previously identified as a recurrent abnormality in T-ALL,[48] it is likely that they cooperate in *SET-NUP214*–mediated leukemogenesis. Nevertheless, the target genes of this aberration remain to be identified.

In conclusion, we identified *SET-NUP214* as a novel recurrent fusion gene in T-cell leukemia. Our experiments show that *SET-NUP214* may contribute to T-ALL pathogenesis by inhibition of T-cell maturation through the transcriptional activation of the *HOXA* genes.

Acknowledgments

This study was supported in part by the Ter Meulen Fund, Royal Netherlands Academy of Arts and Sciences, and the Foundation "De Drie Lichten." P.V.V. is financed by the Sophia Foundation for Medical Research (SSWO-440), M.v.G. was financially supported

by the Quality of Life and KOCR foundations, C.L. was supported in part by a National Cancer Institute grant (CA11560) and a Leukemia and Lymphoma Society Translational grant (6161-05), and J.T. was supported by a German Research Foundation Fellowship Award (Tc-57/1-1).

Authorship

Contribution: P.V.V., J.T., and M.v.G. designed and performed research and wrote the paper; C.L. collaborated on the array-CGH study and wrote the paper; E.v.W. and M.H. collected and made available patient samples; J.G. performed and designed FISH analysis; P.J.S. and A.S. analyzed gene expression data; K.N. and M.F. provided antisera; J.C. and J.S. designed research and wrote the paper; and J.P.P.M, H.B.B., and R.P. wrote the grant, designed research, and wrote the paper.

Conflict-of-interest disclosure: The authors declare no competing financial interests.

Correspondence: Jules P. P. Meijerink, Erasmus MC/Sophia Children's Hospital, Department of Pediatric Oncology/Hematology, Rm Sp 2456, Dr Molewaterplein 60, PO Box 2060, 3000 CB Rotterdam, the Netherlands; e-mail: j.meijerink@erasmusmc.nl.

References

1. Pui CH, Relling MV, Downing JR. Acute lymphoblastic leukemia. N Engl J Med. 2004;350:1535-1548.
2. Clappier E, Cuccuini W, Kalota A, et al. The C-MYB locus is involved in chromosomal translocation and genomic duplications in human T-cell acute leukemia (T-ALL), the translocation defining a new T-ALL subtype in very young children. Blood. 2007;110:1251-1261.
3. Armstrong SA, Look AT. Molecular genetics of acute lymphoblastic leukemia. J Clin Oncol. 2005;23:6306-6315.
4. De Keersmaecker K, Marynen P, Cools J. Genetic insights in the pathogenesis of T-cell acute lymphoblastic leukemia. Haematologica. 2005; 90:1116-1127.
5. Grabher C, von Boehmer H, Look AT. Notch 1 activation in the molecular pathogenesis of T-cell acute lymphoblastic leukaemia. Nat Rev Cancer. 2006;6:347-359.
6. Graux C, Cools J, Melotte C, et al. Fusion of NUP214 to ABL1 on amplified episomes in T-cell acute lymphoblastic leukemia. Nat Genet. 2004; 36:1084-1089.
7. Weng AP, Ferrando AA, Lee W, et al. Activating mutations of NOTCH1 in human T cell acute lymphoblastic leukemia. Science. 2004;306: 269-271.
8. Soulier J, Clappier E, Cayuela JM, et al. HOXA genes are included in genetic and biologic networks defining human acute T-cell leukemia (T-ALL). Blood. 2005;106:274-286.
9. Lahortiga I, De Keersmaecker K, Van Vlierberghe P, et al. Duplication of the MYB oncogene in T cell acute lymphoblastic leukemia. Nat Genet. 2007; 39:593-595.
10. Speleman F, Cauwelier B, Dastugue N, et al. A new recurrent inversion, inv(7)(p15q34), leads to transcriptional activation of HOXA10 and HOXA11 in a subset of T-cell acute lymphoblastic leukemias. Leukemia. 2005;19:358-366.
11. Graux C, Cools J, Michaux L, Vandenberghe P, Hagemeijer A. Cytogenetics and molecular genetics of T-cell acute lymphoblastic leukemia: from thymocyte to lymphoblast. Leukemia. 2006; 20:1496-1510.
12. Van Vlierberghe P, van Grotel M, Beverloo HB, et al. The cryptic chromosomal deletion del(11)(p12p13) as a new activation mechanism of LMO2 in pediatric T-cell acute lymphoblastic leukemia. Blood. 2006;108:3520-3529.
13. Clappier E, Cuccuini W, Cayuela JM, et al. Cyclin D2 dysregulation by chromosomal translocations to TCR loci in T-cell acute lymphoblastic leukemias. Leukemia. 2006;20:82-86.
14. Sharma VM, Calvo JA, Draheim KM, et al. Notch1 contributes to mouse T-cell leukemia by directly inducing the expression of c-myc. Mol Cell Biol. 2006;26:8022-8031.
15. Weng AP, Millholland JM, Yashiro-Ohtani Y, et al. c-Myc is an important direct target of Notch1 in T-cell acute lymphoblastic leukemia/lymphoma. Genes Dev. 2006;20:2096-2109.
16. Palomero T, Lim WK, Odom DT, et al. NOTCH1 directly regulates c-MYC and activates a feed-forward-loop transcriptional network promoting leukemic cell growth. Proc Natl Acad Sci U S A. 2006;103:18261-18266.
17. Ferrando AA, Neuberg DS, Staunton J, et al. Gene expression signatures define novel oncogenic pathways in T cell acute lymphoblastic leukemia. Cancer Cell. 2002;1:75-87.
18. Dik WA, Brahim W, Braun C, et al. CALM-AF10+ T-ALL expression profiles are characterized by overexpression of HOXA and BMI1 oncogenes. Leukemia. 2005;19:1948-1957.
19. Ferrando AA, Armstrong SA, Neuberg DS, et al. Gene expression signatures in MLL-rearranged T-lineage and B-precursor acute leukemias: dominance of HOX dysregulation. Blood. 2003; 102:262-268.
20. Cauwelier B, Cave H, Gervais C, et al. Clinical, cytogenetic and molecular characteristics of 14 T-ALL patients carrying the TCRbeta-HOXA rearrangement: a study of the Groupe Francophone de Cytogenetique Hematologique. Leukemia. 2007;21:121-128.
21. van Grotel M, Meijerink JP, Beverloo HB, et al. The outcome of molecular-cytogenetic subgroups in pediatric T-cell acute lymphoblastic leukemia: a retrospective study of patients treated according to DCOG or COALL protocols. Haematologica. 2006;91:1212-1221.
22. Huber W, von Heydebreck A, Sultmann H, Poustka A, Vingron M. Variance stabilization applied to microarray data calibration and to the quantification of differential expression. Bioinformatics. 2002;18:S96-S104.
23. Hochberg Y, Benjamini Y. More powerful procedures for multiple significance testing. Stat Med. 1990;9:811-818.
24. Barrett MT, Scheffer A, Ben-Dor A, et al. Comparative genomic hybridization using oligonucleotide microarrays and total genomic DNA. Proc Natl Acad Sci U S A. 2004;101:17765-17770.
25. Bernad R, van der Velde H, Fornerod M, Pickersgill H. Nup358/RanBP2 attaches to the nuclear pore complex via association with Nup88 and Nup214/CAN and plays a supporting role in CRM1-mediated nuclear protein export. Mol Cell Biol. 2004;24:2373-2384.
26. Bracken AP, Dietrich N, Pasini D, Hansen KH, Helin K. Genome-wide mapping of Polycomb target genes unravels their roles in cell fate transitions. Genes Dev. 2006;20:1123-1136.
27. Wadman IA, Osada H, Grutz GG, et al. The LIM-only protein Lmo2 is a bridging molecule assembling an erythroid, DNA-binding complex which includes the TAL1, E47, GATA-1 and Ldb1/NLI proteins. EMBO J. 1997;16:3145-3157.
28. Ben-Bassat H, Shlomai Z, Kohn G, Prokocimer M. Establishment of a human T-acute lymphoblastic leukemia cell line with a (16;20) chromosome translocation. Cancer Genet Cytogenet. 1990;49:241-248.
29. von Lindern M, Breems D, van Baal S, Adriaansen H, Grosveld G. Characterization of the translocation breakpoint sequences of two DEK-CAN fusion genes present in t(6;9) acute myeloid leukemia and a SET-CAN fusion gene found in a case of acute undifferentiated leukemia. Genes Chromosomes Cancer. 1992;5: 227-234.
30. Shimoyama T, Kato K, Miyaji-Yamaguchi M, Nagata K. Synergistic action of MLL, a TRX protein with template activating factor-I, a histone chaperone. FEBS Lett. 2005;579:757-762.
31. Seo SB, McNamara P, Heo S, Turner A, Lane WS, Chakravarti D. Regulation of histone acetylation and transcription by INHAT, a human cellular complex containing the set oncoprotein. Cell. 2001;104:119-130.
32. Okada Y, Jiang Q, Lemieux M, Jeannotte L, Su L, Zhang Y. Leukaemic transformation by CALM-AF10 involves upregulation of Hoxa5 by hDOT1L. Nat Cell Biol. 2006;8:1017-1024.
33. Okada Y, Feng Q, Lin Y, et al. hDOT1L links histone methylation to leukemogenesis. Cell. 2005; 121:167-178.
34. Mueller D, Bach C, Zeisig D, et al. A role for the MLL fusion partner ENL in transcriptional elongation and chromatin modification. Blood. 2007;110: 4445-4454.
35. Kritsov A, Feng Z, Lemieux M, et al. Global increase in H3K79 dimethylation in murine and human MLL-AF4 lymphoblastic leukemias [abstract]. Blood. 2007;110: abstract no. 344.
36. Fornerod M, Boer J, van Baal S, Morreau H, Grosveld G. Interaction of cellular proteins with the leukemia specific fusion proteins DEK-CAN and SET-CAN and their normal counterpart, the nucleoporin CAN. Oncogene. 1996;13:1801-1808.
37. Saito S, Miyaji-Yamaguchi M, Nagata K. Aberrant intracellular localization of SET-CAN fusion protein, associated with a leukemia, disorganizes nuclear export. Int J Cancer. 2004;111: 501-507.
38. von Lindern M, Poustka A, Lerach H, Grosveld G. The (6;9) chromosome translocation, associated with a specific subtype of acute nonlymphocytic leukemia, leads to aberrant transcription of a target gene on 9q34. Mol Cell Biol. 1990;10:4016-4026.
39. Rosati R, La Starza R, Barba G, et al. Cryptic chromosome 9q34 deletion generates TAF-Ialpha/CAN and TAF-Ibeta/CAN fusion transcripts in acute myeloid leukemia. Haematologica. 2007; 92:232-235.
40. von Lindern M, Fornerod M, van Baal S, et al. The translocation (6;9), associated with a specific subtype of acute myeloid leukemia, results

in the fusion of two genes, dek and can, and the expression of a chimeric, leukemia-specific dek-can mRNA. Mol Cell Biol. 1992;12:1687-1697.

41. Kandilci A, Mientjes E, Grosveld G. Effects of SET and SET-CAN on the differentiation of the human promonocytic cell line U937. Leukemia. 2004;18:337-340.
42. Saito S, Nouno K, Shimizu R, Yamamoto M, Nagata K Impairment of erythroid and megakaryocytic differentiation by a leukemia-associated and t(9;9)-derived fusion gene product, SET/TAF1b-CAN/NUP214. J Cell Physiol. 2007.
43. Taghon T, Stolz F, De Smedt M, et al. HOX-A10 regulates hematopoietic lineage commitment: evidence for a monocyte-specific transcription factor. Blood. 2002;99:1197-1204.
44. Taghon T, Thys K, De Smedt M, et al. Homeobox gene expression profile in human hematopoietic multipotent stem cells and T-cell progenitors: implications for human T-cell development. Leukemia. 2003;17:1157-1163.
45. Thorsteinsdottir U, Sauvageau G, Hough MR, et al. Overexpression of HOXA10 in murine hematopoietic cells perturbs both myeloid and lymphoid differentiation and leads to acute myeloid leukemia. Mol Cell Biol. 1997;17:495-505.
46. Kroon E, Krosl J, Thorsteinsdottir U, Baban S, Buchberg AM, Sauvageau G. Hoxa9 transforms primary bone marrow cells through specific collaboration with Meis1a but not Pbx1b. EMBO J. 1998;17:3714-3725.
47. Ozbek U, Kandilci A, van Baal S, et al. SET-CAN, the product of the t(9;9) in acute undifferentiated leukemia, causes expansion of early hematopoietic progenitors and hyperproliferation of stomach mucosa in transgenic mice. Am J Pathol. 2007; 171:654-666.
48. Mullighan CG, Goorha S, Radtke I, et al. Genome-wide analysis of genetic alterations in acute lymphoblastic leukaemia. Nature. 2007; 446:758-764.